Calcium carbonates: Induced biomineralization with controlled macromorphology

Aileen Meier[1], Anne Kastner[1], Dennis Harries[2], Maria Wierzbicka-Wieczorek[3], Juraj Majzlan[3], Georg Büchel[4], Erika Kothe[1]

[1]Institute of Microbiology, Friedrich Schiller University Jena, Neugasse 25, 07743 Jena, Germany
[2]Institute of Geosciences, Friedrich Schiller University Jena, Analytical Mineralogy, Carl-Zeiss-Promenade 10, 07745 Jena, Germany
[3]Institute of Geosciences, Friedrich Schiller University Jena, General & Applied Mineralogy, Carl-Zeiss-Promenade 10, 07745 Jena, Germany
[4]Institute of Geosciences, Friedrich Schiller University Jena, Applied Geology, Burgweg 11, 07749 Jena, Germany

Correspondence to: Prof. Dr. Erika Kothe (erika.kothe@uni-jena.de)

Abstract. Biomineralization of (magnesium) calcite and vaterite by bacterial isolates has been known for quite some time. However, the extracellular precipitation hardly has been linked to different mophologies of the minerals that are observed. Here, isolates from limestone associated groundwater, rock and soil were shown to form calcite; magnesium calcite or vaterite was also present. More than 92 % of isolates indeed could form carbonates, while abiotic controls failed in mineral formation. The crystal morphologies varied, including rhombohedra, prisms and pyramid-like macro-morphologies. Using different conditions like varying temperature, pH or media components, but also co-cultivation to test for collaborative effects of sympatriotic bacteria, were used to differentiate mechanisms of calcium carbonate formation. Single crystallites were cemented with bacterial cells; these may have served as nucleation sites by providing a basic pH at short distance from the cells. A calculation of potential calcite formation of up to 2 g per liter of solution could link the microbial activity to geological processes.

1 Introduction

The processes of carbonate biomineralization by bacteria are usually linked to an alkaline microenvironment enhancing the potential for carbonate precipitation at small spatial scales (Hammes and Verstraete, 2002). By uptake of CO_2, precipitation of calcium carbonates is favored, especially in presence of Ca^{2+}. Thus, the process clearly may be defined as microbially induced biomineralization, in contrast to microbially controlled processes best seen with intracellular, compartment-bound formation of magnetite by magnetotactic bacteria. The cell surface can act as a nucleation site for mineralization (Schultze-Lam et al., 1996). Since properties are different for Gram positives and Gram negatives, both binding divalent cations such as Mg^{2+} or Ca^{2+}, a determination of the microbial clades is necessary (Chahal et al., 2011; Douglas and Beveridge, 1998; Zhu et al., 2017). Depending on different cell surface structures, different crystal morphologies have been reported (Cao et al., 2016; Seifan et al., 2016). Nevertheless, even from one and the same bacterial isolate, different macro-morphologies of

biominerals were described (Tisato et al., 2015). Thus, a more thorough investigation of microbially induced biomineralization seems warranted.

The occurrence of carbonate forming bacteria has been investigated with respect to different environments (Andrei et al., 2017; Gray and Engels, 2013; Horath and Bachofen, 2009; Kang and Roh, 2016; Rusznyak et al., 2012). The process generally was linked to changes induced in the direct microenvironment of the growing bacteria through metabolic features, or to providing nucleation sites for crystallization in a supersaturated environment (Roberts et al., 2013; Seifan et al., 2017; Yan et al., 2017). Either microbiomes of a specific habitat, or physiological and biomineralization properties of a single isolate have been investigated. To bridge that gap, an investigation of more isolates from one environment seems indicated.

As a result of growing knowledge on carbonate biomineralization, applications in concrete repair and formulation of self-healing cement have been derived (Achal et al., 2009; Li et al., 2017; Seifan et al., 2016; Singh et al., 2015). Additionally, carbonate formation for remediation purposes has gained interest (Kumari et al., 2016; Zhu et al. 2016), including wastewater treatment (Gonzalez-Martinez et al., 2017).

Basic scientific questions addressed include the nature and rates of biotic *versus* abiotic nature of calcite formation. For one species, 33 g/L calcite precipitation was reported (Seifan et al., 2016). The same assumption has been tested for the formation of rhodoliths in marine systems, where carbonate rocks evolve (Cavalcanti et al., 2014). The formation of CO_2 through respiration clearly is a factor that would imply aerobic microbes (Keiner et al., 2013). Hence, a marine sediment derived limestone habitat and isolation of aerobic bacteria from that environment seemed indicated (compare Meier et al., 2017).

We thus were interested to identify different bacteria from a carbonate rock-water-soil system to address the question of how bacteria may contribute to different morphologies, even at a distance to the cells, and how much calcium carbonates may be formed *in vitro* under conditions more likely to occur in nature than previously used (Castanier et al., 1999). To obtain a variety of calcium carbonate forming bacterial isolates, we focused on marine Triassic limestones exposed in central Germany. We obtained Gram-positive and Gram-negative bacteria from the limestones, groundwater and rendzina soil developed on the limestones near the limestone quarry Bad Kösen (Thuringia, Germany). The isolated bacteria represented major taxa present in the microbiomes (Meier et al., 2017). They were incubated in single culture or in co-cultivation under different conditions to address biomineralization relevant to carbonate formation. With our results, we can advance the background on microbially induced biomineralization with respect to different mechanisms.

2 Material and Methods

2.1 Sampling

The Muschelkalk quarry in Bad Kösen is characterized by Lower Muschelkalk (Jena Formation, Lower Wellenkalk core sampled) and Middle Muschelkalk (Karstadt Formation, upper Schaumkalkbank sampled). Rock samples were taken from cores under sterile conditions.

The groundwater wells near Bad Kösen, in Stöben (Hy Camburg 13/198; 4478864N, 5660183E; Lower Muschelkalk sampled at 34 m depth) and Wichmar (Hy Camburg 121/1988; 4478030N, 5655906E; 120 m, Middle Muschelkalk sampled at 17 m) were sampled with the help of an electric pump after reaching constant pH and temperature. All samples were stored at 6 °C prior to analysis.

Soil was sampled at 40 cm depth from 15 sampling points at the Bad Kösen quarry for rendzina on the respective limestone bed in a radius of about 1 km and homogenized.

2.2 Isolation and characterization of bacteria

For the isolation of bacteria from the limestones, Std I (Carl Roth; supplied with NaCl at 3, 5, 7 % if indicated by sample chemistry), minimal AM (Amoroso et al., 2002) and oligotrophic R_2A (Reasoner and Geldreich, 1985) media were applied. Calcification promoting B-4 medium without pH adjustment (Banks et al., 2010) was used for isolating limestone associated bacteria.

For rock samples, 5 g of powdered rock sample were added to 45 ml sterile 0.9 % NaCl, followed by vortexing for 20 min. Subsequently, sonication was applied for 15 min and filtered supernatant was plated.

A total of 2.5 L of groundwater samples were filtered before culturing using 0.2 µm membrane filters (Omnipore membrane filters, Millipore) in a filtration system (GP Millipore Express plus membrane, Millipore). The filters were placed on agar and incubated at 10 °C for three days. Additionally, dilution series in sterile 0.9 % NaCl solution were plated. Surface sterilized rock samples were powdered and dilution series were prepared, cultured in liquid medium or placed as small particles on nutrient agar.

Soil extracts from 100 g mixed soil samples, dried at 40 °C overnight were prepared using 500 ml 10 mM 3-(N-morpholino)propansulfonic acid (MOPS, Serva). The suspension was incubated at 28 °C for 1 hour prior to filtration with a vacuum pump system. The extract was supplemented with 100 mg/L glucose, 1 mg/L casein hydrolysate, 1 mg/L yeast extract and 18 mg/L agar and sterilized before adding to cultures obtained from rock and soil samples. Incubation was performed at 28 °C and 10 °C for 3 to 5 days in duplicates, with constant shaking at 120 rpm for liquid cultures.

For strain identification, genomic DNA was extracted from pure cultures and 16S rDNA was amplified (primers 27F and 1492r at 100 mM, 0.02 U Dream Taq polymerase, 1 x Dream Taq buffer, 100 mM deoxynucleotide triphosphate mixture, 1 µl DNA template) with 30 cylces (95 °C for 3 min, followed by cycles of 95 °C for 30 sec, 57-60 °C for 30-45 sec, 72 °C for 60-90 sec, with final step at 72 °C for 10-30 min) and sequenced (GATC Biotech, Konstanz). The obtained sequences were assembled *via* Bioedit sequence alignment editor version 7.1.3.0 and analyzed using NCBI BLAST tool (http://www.ncbi.nlm.nih.gov, see also supplemental Tab. S1). All obtained sequences were made available with NCBI GenBank (see Meier et al., 2017). The strains are deposited with the Jena Microbial Ressource Collection.

2.3 Biomineralization assays

To study effects on carbonate mineralization, B-4 agar plates or liquid cultures were incubated at 28 °C or 10 °C for one to three weeks. $CaCO_3$ (B-4CO) or $Ca_3(PO_4)_2$ (B-4CP) as source of calcium were used replacing the calcium acetate of the medium. For differentiation between biological and chemical mechanisms, non-inoculated plates and plates streaked with dead biomass were used as negative controls. Bromthymol blue (Merck, Darmstadt) was used as pH indicator where appropriate.

Selected experiments were designed to investigate competition or induction of activities of the bacterial strains streaked towards each other on B-4 agar. Two- or four-strain interactions were tested using compatriot isolates from the same habitat.

2.4 Mineralogical investigations

Solid products were visualized with a stereomicroscope (Zeiss) and sampled in 0.2 ml reaction tubes. Powder X-ray diffractometer (Bruker D8 Advance) with Cu Kα radiation (λ=1.54058 Å) and LynxEye detector was used on powdered crystals transferred to a zero-background silicon sample holder and measured with following parameters: 18-70 °2θ, a step size of 0.02 º2Θ and dwell of 0.5 sec.

Scanning electron micrographs (SEM; Quanta 3D FEG; FEI) were taken from carbon or gold sputtered samples imaged in secondary (SE) or back-scattered electron mode (BSE) at an acceleration voltage of typically 10 kV. Semi-quantitative chemical analysis was conducted using an energy-dispersive X-ray (EDX) spectrometer (EDAX, Mahwah).

2.5 Quantification of precipitate formation

Liquid medium inoculated with *Agrococcus jejuensis* sMM51, *Bacillus muralis* rLMd or *Bacillus sp*. rMM9 was incubated at 28 °C for at least three weeks. Precipitates were harvested using a sterile cell strainer (easystrainer, 40µm for 50 ml tubes, GBO) and rinsed with pure water to separate cells from the solids. The crystals were dried and weighed. Bacterial growth was determined with cells diluted 1:1000 with ISOTON Diluent (Beckman Coulter, Brea) in a Coulter cell counter in triplicates.

For calcultation of yearly biomineral formation, we used the amount produced in our cultures (approx. 100 mg) during the time of incubation (3 weeks) to calculate how much this would make in 52 weeks, a full year. 1700 mg would be the result of such an approximate calculation for new mineral formation during a year. This is an underestimation, since the nucleation time is needed only once.

3. Results

3.1 Biomineralization activities of bacterial isolates

This study is focused on bacterial isolates from two different limestones, Lower Muschelkalk (LM) and Middle Muschelkalk (MM), and three compartments for each lithotype representing rock (r), groundwater (gw) and soil (s). Of 140 isolates, only 10 formed no crystals under the conditions tested (Figs. 1-6). This shows that in a carboniferous environment, strains forming carbonates are highly enriched.

As to the means of inducing mineralization, the influence of pH could be tested. While 89 strains did not change medium pH, 43 produced an alkaline environment supportive of carbonate formation. However, two of those alkalinity producing strains did not produce biominerals, all other non-producers did not change pH. In addition, crystal formation was observed with all strains which actually lowered pH. The temperature clearly had an effect, although there was no clear correlation. While on one medium, higher temperature might have induced formation of crystals not observed at low temperature, the opposite effect was visible on the next medium. Any combination of traits was observed. This indicates that rather differences among strains than a mere general influence on the micro-environmental conditions leading to abiotic carbonate formation was observed.

The highest incidence of mineral production was observed with soil isolates obtained from soil developed on Middle Muschelkalk. Biomineralization potential was not associated to phylogeny. Eight isolates of the genus *Bacillus* isolated from Lower Muschelkalk rock samples induced precipitation, whereas six strains of the same genus were negative in biomineralization.

3.2 Identification of calcium carbonate biominerals

From each habitat, the four most prevalent isolates were selected for further study (Tab. 1). Of these 24 strains, 16 were Gram positives, representing the taxa *Agrococcus, Arthrobacter, Bacillus, Micrococcus, Planococcus, Psychrobacillus, Rhodococcus* and *Streptomyces.* The eight Gram negative genera were *Advenella, Agromyces, Flavobacterium, Lelliottia, Moraxella, Ochrobactrum, Pseudomonas,* and *Sphingopyxis.* There was no correlation between medium or temperature preference and biomineralization visible.

Powder X-ray diffraction and EDX analyses identified mostly calcite, less frequently vaterite and magnesium calcite (see Tab. 1). Calcite formed on cultures from rock of Lower Muschelkalk *Bacillus sp.* rLMa, *Micrococcus luteus* rLMc and *B. muralis* rLMd and Middle Muschelkalk *Agrobacter pascens* rMM19 and *Ochrobactrum intermedium* rMM23. Of these, *B. muralis* rLMd and *Agrobacter pascens* rMM19 concomitantly formed vaterite. No magnesium calcite was found with strains isolated from rock samples. The groundwater isolates showed lowest incidence but high variability of biomineralization with *Arthrobacter sp*. W_2.1 forming vaterite, while *Advenella sp.* W_Sd3 and *Rhodococcus erythropolis* W_Sd5 were found to form vaterite and magnesium calcite. All three phases were present in one example, a strain obtained from soil of Lower Muschelkalk, *Streptomyces sp.* SLM5. Soil isolates from Middle Muschelkalk *Streptomyces sp.* sMM10 and *Sphingopyxis*

bauzanensis sMM41 formed vaterite and magnesium calcite, while *Agrococcus jejuensis* sMM crystallized calcite and vaterite.

3.3 Variation in crystal morphologies

Color and morphology of crystal aggregates were highly variable, ranging from colorless to brownish or purple, and morphologies from individual rhombohedral crystals, round or acicular aggregates or rosettes to laminated crusts. Aggregates located within the agar mostly formed small rhombohedra or spheres.

Biominerals were on top or below the biomass; for some strains the crystals formed always in a certain distance from the colonies, which might indicate a zone of change in pH around the culture (Fig. 7). Indicator plates with bromthymol blue indicated mainly change to basic pH > 7.6, followed by crystal precipitation. A few isolates of each environment revealed acidification, most pronounced for Lower Muschelkalk *Bacillus* strains and Middle Muschelkalk *Streptomyces* with pH < 6.0.

A recurring morphological feature was subparallel intergrowth of µm to sub-µm sized crystallites. In simple cases, the resulting aggregates resembled the morphology of a single crystal, in other cases, more complex aggregates were found (Fig. 8; for further morphologies of other isolates, see supplemental Fig. S1). Crystal aggregates produced by *L. amnigena* S_H3 exhibited platy crystals arranged into a rosette.

3.4 Impact of cultivation conditions

Phenotypic differences in crystal morphology were readily observed, dependent also on temperature (Fig. 9). On plates containing calcium carbonate or calcium phosphate, more bacterial growth, but less biomineralization was observed. On the medium with $CaCO_3$, the groundwater isolates showed temperature-dependent biomineralization. Crystals were formed at 10 °C, whereas the temperature of 28 °C induced mineral dissolution indicated by halo formation.

3.5 Direct impact of bacteria

The bacterial influence was visible also by direct associations. *R. erythropolis* WSd5 crystals were coated by bacterial cells (see Fig. 8). Some areas free of cells contained oval, clearly delimited holes of the same size and shape as the surrounding bacterial cells. Occasionally, these holes were characterized by an extended trace (a tail) on one side.

Two or four strains of one community were co-cultivated to determine their interactions. There was either no interaction, inhibition leading to lack of growth, or parasitism visible by overgrowing the competing strain(s). Concerning biomineralization, the co-cultivation had either no effect, or it enhanced precipitation, producing larger crystals in the contact zone (Tab. 2). The biotic interactions showed an impact on biomineralization, e.g. with *L. amnigena* S_H3 with more crystals developing at the contact zones, *Advenella sp.* W_Sd3 from groundwater of Middle Muschelkalk was overgrown by all interaction partners without a change in crystal distribution, and *Streptomyces sp.* sLM17 from the Middle Muschelkalk rock sample inhibited *A. cerinus* sLM10 without crystal formation.

3.6 Quantification of precipitates

The quantification of crystals formed resulted in similar cell counts ranging from $2.06 * 10^7$ to $8.65 * 10^7$. Since the bacterial biomass within the centrifugation pellet thus was similar, the dry mass was compared to see different rates of biomineral formation. The dry weight of precipitates varied, with highest amounts and thus the highest ability for crystal formation seen with *Bacillus sp.* rMM9 (0.104 g/L), followed by *Agrococcus jejuensis* sMM 51 (0.096 g/L). *Bacillus muralis* rLMd demonstrated the lowest amount of crystals wit 0.064 g/L (Tab. 3).

4. Discussion

Microbially induced calcite precipitation has been known as a general phenomenon since the 1970's and found application in different fields such as cementation of cracks in historical memorials, buildings or sculptures made of limestone by cementing cracks, mostly through ureolytic bacteria (van Tittelboom et al., 2010; Wong, 2015; Zhu and Dittrich, 2016). The general availability of bacterial isolates from different environments associated with limestones, however, was not accessed to the full (Gonzales-Martinez et al., 2017; Seifan et al., 2017). Here, two lithotypes of Lower and Middle Muschelkalk were assessed for the prevalence of carbonate precipitating bacteria.

Calcite, magnesium calcite and vaterite could be formed by the bacteria growing on standard laboratory media. Since vaterite occurs in aqueous, supersaturated solutions, high water content in the precipitates might be explained with water available from the agar. Magnesium calcite was likely formed when the bacterial cell surfaces accumulated the element (see also Cui et al., 2015; Rusznyak et al., 2012). Few trace elements, such as sulfur, chloride and phosphorus probably originating from cell components or salts included in the medium have been detected (see also Rivadeneyra et al., 2000).

Different crystal aggregates with macro-morphologies such as rhombohedra, rosettes and spheres were detected, occurring either in the medium at a distance to the inoculated bacteria, or below or on top of the cultures. Morphological variations of crystal shapes revealed a microbial impact on mineral precipitation (compare Branson et al., 2016). Crystal colors by impurities incorporated in the lattice such as salts or secreted pigments were clearly observed, as calcite can incorporate metal ions in its crystal structure (Kang et al., 2014).

With respect to alkaline pH favorable for calcium carbonate precipitation, a probable process might be the ammonification of amino acids, deriving from yeast extract added to the medium. By degrading amino acids, ammonia develops which increases the pH to alkaline conditions. So far, mostly urease activity has been implied for pH increase in biogenic calcite formation (Bachmeier et al., 2002; Okyay et al. 2016; Wei-Soon et al., 2012). However, our results with strains acidifying the medium and still precipitating calcium carbonate clearly shows that other mechanisms are involved as well.

Biotic effects were investigated by co-cultivation. Growth inhibition of a compatriote strain could be a result of secreted antimicrobial compounds or competition (Hibbing et al., 2009). Growth promotion, like with *Flavobacterium limicola* S_5.3, may be due to growth promoting compounds for interspecies communication of xenosiderophore use. Increased

crystallization at contact zones was noticed in specific bacterial combinations, e.g. with *Rhizobium sp*. S_4.1a and *Pseudomonas sp.* S_H4.

Biogenic calcite precipitation may contribute to limestone sedimentation (compare Garcia et al., 2016). With 0.104 g/L dry weight for *Bacillus sp.*rMM9, a high yield of carbonate precipitation was found. Bacterial cells, especially spores with their high surface to volume ratio and specific cell wall structure, can serve as nucleation sites. Spores encapsulated by calcite might survive for long periods of time, and can be reactivated, followed by germination and growth of new bacterial generations (Murai and Yoshida, 2013). Hence, ample sporulation may explain differences in the amounts recorded between different strains of the genus *Bacillus* (Yasuda-Yasaki et al., 1978).

Bacteria are known to contribute to the growth of carbonate stalactites that grow by a few mm per year (Genty et al., 2011). Comparing these observations to our experiment, bacterial isolates may exert a meaningful impact on limestone deposition. From the 104 mg/L after three weeks, up to yearly 2 g/L can be calculated. This compares well to a model experiment which resulted in ~ 2 g abiotic $CaCO_3$/yr (Short et al., 2005). As we could show increase in productivity in mutual interactions, microbial communities might well reach even higher rates (Castanier et al., 1999).

As a main result of our investigation of 140 isolates of two lithotypes of limestone in Germany, we can conclude that (magnesium) calcite and vaterite production can be induced through medium alkalinity, through direct surface interation for nucleation visible in close associations, but also in acidified media and a distance apart from the growing bacteria. This indicates, that within the microbially induced calcium carbonate precipitation, mechanistically different routes of biomineralization are possible. The control of morphologies at a distance to the colony seems specifically interesting. We propose that molecules secreted by the bacteria, e.g. specific proteins, might lead to preferential crystal growth at different mineral surfaces due to coating. This clearly warrants further, more molecular studies.

Acknowledgements

The authors would like to thank Falko Langenhorst, Dirk Merten, Thomas Wach, Hans-Martin Dahse and Justus Linden for help with measurements. The International Max-Planck Research School "global Biogeochemical Cycles" and the Jena School for Microbial Communication (GSC124) are thanked for financial support. EK wishes to acknowledge DFG-CRC 1127.

References

Achal, V., Mukherjee, A., Basu, P.C., and Reddy, M.S.: Strain improvement of *Sporosarcina pasteurii* for enhanced urease and calcite production, J. Ind. Microbiol. Biotechnol., 36, 981-988, 2009.

Amoroso, M.J., Schubert, D., Mitscherlich, P., Schumann, P., and Kothe, E.: Evidence for high affinity nickel transporter genes in heavy metal resistant *Streptomyces spec*., J. Basic Microbiol., 40, 295-301, 2000.

Andrei, A.S., Pausan, M.R., Tamas, T., Har, N., Barbu-Tudoran, L., Leopold, N., and Manciu, H.L.: Diversity and biomineralization potential of the epilithic bacterial communities inhabiting the oldest public stone monument of Cluj-Napoca (Transylvania, Romania), Front. Microbiol., 8, 372, 2017.

Bachmeier, K.L., Williams, A.E., Bang, S.S., and Warmington, J.R.: Urease activity in microbiologically-induced calcite precipitation, J. Biotechnol. 93, 171–181, 2002.

Banks, E.D., Taylor, N.M., Gulley, J., Lubbers, B.R., Giarrizzo, J.G., Bullen, H.A., Hoehler, T.M., and Barton, H.A.: Bacterial calcium carbonate precipitation in cave environments: A function of calcium homeostasis, Geomicrobiol. J. 27, 444-454. 2010.

Branson, O., Bonnin, E.A., Perea, D.E., Spero, H.J., Zhu, Z., Winters, M., Hönisch, B., Russell, A.D., Fehrenbacher, J.S., and Gagnon, A.C.: Nanometer-scale chemistry of a calcite biomineralization template: Implications for skeletal composition and nucleation, Proc. Natl. Acad. Sci. U.S.A. 113, 12934-12939, 2016.

Castanier, S., Le Métayer-Levrel, G., and Perthuisot, J.-P.: Ca-carbonates precipitation and limestone genesis - the microbiogeolist point of view, Sediment. Geol. 126, 9-23. 1999.

Chahal, N., Rajor, A., and Siddique, R.: Calcium carbonate precipitation by different bacterial strains, Afric. J. Biotechnol. 10, 8359-8372, 2011.

Cao, C., Jiang, J., Sun, H., Huang, Y., Tao, F., and Lian, B.: Carbonate mineral formation under the influence of limestone-colonizing actinobacteria: Morphology and polymorphism, Front. Microbiol. 7, 366, 2016.

Cavalcanti, G.S., Gregoracci, G.B., dos Santos, E.O., Silveira, C.B., Meirelles, P.M., Longo, L., Gotoh, K., Nakamura, S., Iida, T., Sawabe, T., Rezende, C.E., Francini-Filho, R.B., Moura, R.L., Amado-Filho, G.M., and Thompson, F.L.: Physiologic and metagenomic attributes of the rhodoliths forming the largest $CaCO_3$ bed in the South Atlantic Ocean, ISME J. 8, 52-62. 2014.

Cui, J., Kennedy, J.F., Nie, J., and Ma, G.: Co-effects of amines molecules and chitosan films on in vitro calcium carbonate mineralization, Carbohydr. Polym. 133, 67-73, 2015.

Douglas, S., and Beveridge, T.J.: Mineral formation by bacteria in natural microbial communities, FEMS Microbiol. Ecol. 26, 79-88, 1998.

García, G.M., Márquez, G.M.A., and Moreno, H.C.X.: Characterization of bacterial diversity associated with calcareous deposits and drip-waters, and isolation of calcifying bacteria from two Colombian mines, Microbiol. Res. 182, 21-30, 2016.

Genty, D., Baker, A., and Vokal, B.: Intra- and inter-annual growth rate of modern stalagmites, Chem. Geol. 176, 191–212, 2011.

Gonzalez-Martinez, A., Rodriguez-Sanchez, A., Rivadeneyra, M.A., Rivadeneyra, A., Martin-Ramos, D., Vahala, R., and Gonzalez-Lopez, J.: 16S rRNA gene-based characterization of bacteria potentially associated with phosphate and carbonate precipitation from a granular autotrophic nitrogen removal bioreactor, Appl. Microbiol. Biotechnol. 101, 817-829. 2017.

Gray, C.J., and Engel, A.S.: Microbial diversity and impact on carbonate geochemistry across a changing geochemical gradient in a karst aquifer, ISME J. 7, 325-337, 2013.

Hammes, F., and Verstraete, W.: Key roles of pH and calcium metabolism in microbial carbonate precipitation, Environ. Sci. Biotechnol. 1, 3-7, 2002.

Hibbing, M.E., Fuqua, C., Parsek, M.R., and Peterson, S.B.: Bacterial competition: surviving and thriving in the microbial jungle, Nature Rev. Microbiol. 8, 15-25, 2009.

Horath, T., and Bachofen, R.: Molecular characterization of an endolithic microbial community in dolomite rock in the central Alps (Switzerland), Microbial Ecol. 58, 290-306, 2009.

Kang, S.K., and Roh, Y.: Microbially-mediated precipitation of calcium carbonate nanoparticles, J. Nansci. Nanotechnol. 16, 1975-1978, 2016.

Kang, C.-H., Han, S.-H., Shin, Y., Oh, S.J., and So, J.-S.: Bioremediation of Cd by microbially induced calcite precipitation, Appl. Biochem. Biotechnol. 172, 2907-2915, 2014.

Keiner, R., Frisch, T., Hanf, S., Rusznyak, A., Akob, D.M., Küsel, K., and Popp, J.: Raman spectroscopy - an innovative and versatile tool to follow the respirational activity and carbonate biomineralization of important cave bacteria, Anal. Chem. 85, 8708-8714, 2013.

Kumari, D., Qian, X.Y., Pan, X., Achal, V., Li, Q., and Gadd, G.M.: Microbially-induced carbonate precipitation for immobilization of toxic metals, Adv. Appl. Microbiol. 94, 79-108, 2016.

Li, M., Zhu, X., Mukherjee, A., Huang, M., and Achal V.: Biomineralization in metakaolin modified cement mortar to improve its strength with lowered cement content, J. Hazard. Mater. 329, 178-184, 2017.

Meier, A., Singh, M.K., Kastner, A., Merten, D., Büchel, G., and Kothe, E.: Microbial communities in carbonate rocks - from soil via groundwater to rocks, J. Basic Microbiol., in press.

Murai, R., and Yoshida, N.: *Geobacillus thermoglucosidasius* endospores function as nuclei for the formation of single calcite crystals, Appl. Environ. Microbiol. 9, 3085-3090, 2013.

Okyay, T.O., Nguyen, H.N., Castro, S.L., and Rodrigues, D.F.: CO_2 sequestration by ureolytic microbial consortia through microbially-induced calcite precipitation, Sci. Total Environ. 572, 671-680, 2016.

Reasoner, D.J., and Geldreich, E.E.: 1985. A new medium for the enumeration and subculture of bacteria from potable water, Appl. Environ. Microbiol. 49, 1-7, 2016.

Rivadeneyra, M.A., Delgado, G., Soriano, M., Ramos-Cormenzana, A., and Delgado, R.: Precipitation of carbonates by *Nesterenkonia halobia* in liquid media, Chemosphere 41, 617-624, 2000.

Roberts, J.A., Kenward, P.A., Fowle, D.A., Goldstein, R.H., Gonzales, L.A., and Moore, D.S.: Surface chemistry allows for abiotic precipitation of dolomite at low temperature, Proc. Natl. Acad. Sci. U.S.A. 110, 14540-14545, 2013.

Rusznyak, A., Akob, D.M., Nietsche, S., Eusterhues, K., Totsche, K.U., Neu, T.R., Frosch, T., Popp, J., Keiner, R., Geletneky, J., Katzschmann, L., Schulze, E.D., and Küsel, K.: Calcite biomineralization by bacterial isolates from the recently discovered pristine karstic Herrenberg cave, Appl. Environ. Microbiol. 78, 1157-1167, 2012.

Schultze-Lam, S., Fortin, D., Davis, B.S., and Beveridge, T.J.: Mineralization of bacterial surfaces, Chem. Geol. 132, 171-181, 1996.

Seifan, M., Samani, A.K., and Berenjian, A.: Bioconcrete: next generation of self-healing concrete, Appl. Microbiol. Biotechnol. 100, 2591-2602, 2016.

Seifan, M., Samani, A.K., and Berenjian, A.: New insights into the role of pH and aeration in the bacterial production of calcium carbonate ($CaCO_3$), Appl. Microbiol. Biotechnol. 101, 3131-3142, 2017.

Short, M.B., Baygents, J.C., Beck, W.J., Stone, D.A., Toomey III, R.S., and Goldstein, R.E.: Stalactite growth as a free-boundary problem: A geometric law and its platonic ideal, Phys. Rev. Lett. 94, 018501, 2005.

Singh, R., Yoon, H., Sanford, R.A., Katz, L., Fouke, B.W., and Werth, C.J.: Metabolism-induced $CaCO_3$ biomineralization during reactive transport in a micromodel: Implications for porosity alteration, Environ. Sci. Technol. 49, 12094-12104, 2015.

Tisato, N., Torriani, S.F., Monteux, S., Saure, F., De Waele, J., Tacagna, M.L., D'Angeli, I.M., Chailloux, D., Renda, M., Eglinton, T.I., and Bontognali, T.R.: Microbial mediation of complex subterranean mineral structures, Sci. Rep. 5, 15525, 2015.

van Tittelboom, K., De Belie, N., De Muynck, W., and Verstraete, W.: Use of bacteria to repair cracks in concrete, Cement Concr. Res. 40, 157-166, 2010.

Wei-Soon, N., Lee, M.-L., and Hii, S.-L.: An overview of the factors affecting microbial-induced calcite precipitation and its potential application in soil improvement, Int. J. Civic Environ. Struct. Constr. Architect 6, 188-194, 2012.

Wong, L.S.: 2015. Microbial cementation of ureolytic bacteria from the genus *Bacillus*: a review of the bacterial application on cement-based materials for cleaner production, J. Cleaner Product 93, 5-17, 2012.

Yan, W., Xiao, X., and Zhang, Y.: Complete genome sequence of *Lysinibacillus sphaericus* LMG 22257, a strain with ureolytic activity inducing calcium carbonate precipitation, J. Biotechnol. 246, 33-35, 2017.

Yasuda-Yasaki, Y., Namiki-Kanie, S., and Hachisuka, Y.: Inhibition of *Bacillus subtilis* spore germination by various hydrophobic compounds: demonstration of hydrophobic character of L-alanine receptor site, J. Bacteriol. 136, 484-490, 1978.

Zhu, T., and Dittrich, M.: Carbonate precipitation through microbial activities in natural environment, and their potential in biotechnology: A review, Front. Bioengin. Biotechnol. 4, 4, 2016.

Zhu, X., Li, W., Zhan, L., Huang, M., Zhang, Q., and Achal, V.: The large-scale process of microbial carbonate precipitation for nickel remediation from an industrial soil, Environ. Pollut. 19, 149-155, 2016.

Zhu, Y., Ma, N., Jin, W., Wu, S., and Sun, C.: Genomic and transcriptomic insnights into calcium carbonate biomineralization by marine actinbacterium *Brevibacterium linens* BS258, Front. Microbiol. 8, 602, 2017.

Table 1: Biomineral identification from strains obtained from groundwater (gw), rock (r) and soil (s) samples from Lower (LM) and Middle Muschelkalk (MM).

Strain	Calcite	Vaterite	Magnesium calcite
rLM			
B. niacini rLM1.4	+	+	-
Bacillus sp. rLMa	+	-	-
Micrococcus luteus rLMc	+	-	-
Bacillus muralis rLMd	+	+	-
rMM			
Bacillus sp. rMM9	+	+	-
Agrobacter pascens rMM19	+	+	-
Ochrobactrum intermedium rMM23	+	-	-
gwLM			
Pseudomonas sp. S_1.1	+	-	-
Microbacterium sp. S_2.10	+	+	-
B. sharmana S_3.1	-	-	+
Rhizobium sp. S_4.1	+	-	-
Rahnella sp. S_H1	+	+	-
gwMM			
Arthrobacter sp. W_2.1	-	+	-
C. koreensis W_5.3b	+	-	+
Flavobacterium sp. W_5.4	+	+	+
Uncultured Leifsonia sp. W_Sd1	-	+	+
Advenella sp. W_Sd3	-	+	+
Rhodococcus erythropolis W_Sd5	-	+	+
sLM			
Streptomyces sp. sLM5	+	+	+
B. frigoritolerans sLM13	-	-	+
Paenibacillus sp. sLM29	+	-	-
sMM			
Streptomyces sp. sMM10	-	+	+
P. umidemergens sMM17	+	-	-
S. maltophilia sMM31	+	+	-
Sphingopyxis bauzanensis sMM41	-	+	+
Bacillus sp. sMM46	-	-	+
Agrococcus jejuensis sMM51	+	+	-

+, detected; -, not detected

Table 2: Growth and biomineralization of compatriote bacterial isolates in co-cultivation from groundwater (gw), rock (r) and soil (s) samples from Lower (LM) and Middle Muschelkalk (MM).

	Growth	Biomineralization
rLM		
Micrococcus luteus rLMc	Inhibited *B. simplex* 3.3F	-
Bacillus muralis rLMd	Highest growth rate, overgrew all interaction strains	-
Bacillus sp. rLMa		-
Bacillus simplex 3.3F	Inhibition by *B. muralis* rLMd	At contact point to *Bacillus sp.* rLMa, increased
rMM		
Bacillus sp. rMM8	Highest growth rate, overgrew *O. intermedium* rMM23	Increased crystal accumulation at contact point to *A. pascens* rMM 19
Agrobacter pascens rMM19	+/-	Crystals at contact point to *Bacillus sp.* rMM8
Psychrobacillus psychrodurans rMM20	+/- near contact point to *Bacillus sp.* rMM8	Crystals at contact point to *Bacillus sp.* rMM8
Ochrobactrum intermedium rMM23		No change in biomineralization
gwLM		
Leliottia amnigena S_H3	Highest growth rate, overgrew competitors	At contact points increased
Pseudomonas sp. S_H4		-
Rhizobium sp. S_4.1a		-
Flavobacterium limicola S_5.3		-
gwMM		
Advenella sp. W_Sd3	Overgrown by all interaction partners	-
Rhodococcus erythropolis W_Sd5	Inhibition by *Planococcus sp.* W_1.2 and *Arthrobacter sp.* W_2.1	-
Planococcus sp. W_1.2	Overgrown by *Arthrobacter sp.* W_2.1 and *R. erythropolis* W_Sd5, inhibition of *R. erythropolis* W_Sd5 at contact point	-
Arthrobacter sp. W_2.1	Highest growth rate, inhibition of W_Sd5 at contact point	Increased crystal accumulation near contact point
sLM		
Streptomyces sp. sLM8		-
Agromyces cerinus sLM10		-
Streptomyces sp. sLM17	Inhibition of *A. cerinus* sLM10	-
Bacillus sp. sLM42	Highest growth rate, overgrew all interaction strains	-
sMM		
Streptomyces sp. sMM10	Highest growth rate, overgrew *M. osloensis* sMM16 and *S. bauzanensis* sMM41	-
Moraxella osloensis sMM16		Increased crystal accumulation at contact point to *Streptomyces sp.* sMM10 and *A. jejuensis* sMM51
Sphingopyxis bauzanensis sMM41		+/-
Agrococcus jejuensis sMM51	Inhibition by *M. osloensis* sMM16	Increased crystal accumulation at contact point to *M. osloensis* sMM16

-, no crystals/no growth; +/-, low amount of crystals or low growth

Table 3: Quantification of calcite precipitation by isolates from rock (r) and soil (s) of Lower (LM) and Middle Muschelkalk (MM). Similar cell counts were obtained. The dry weight of crystals was measured (see Material and Methods).

Strain	Mean Coulter cell counter [cells/ml]	Dry weight [g/L]
***Bacillus muralis* rLMd**	$3.97*10^7$	0.064
***Bacillus sp.*rMM9**	$5.77*10^7$	0.104
***Streptomyces sp.* sLM37**	$2.06*10^7$	0.088
Agrococcus jejuensis sMM51	$8.65*10^7$	0.096

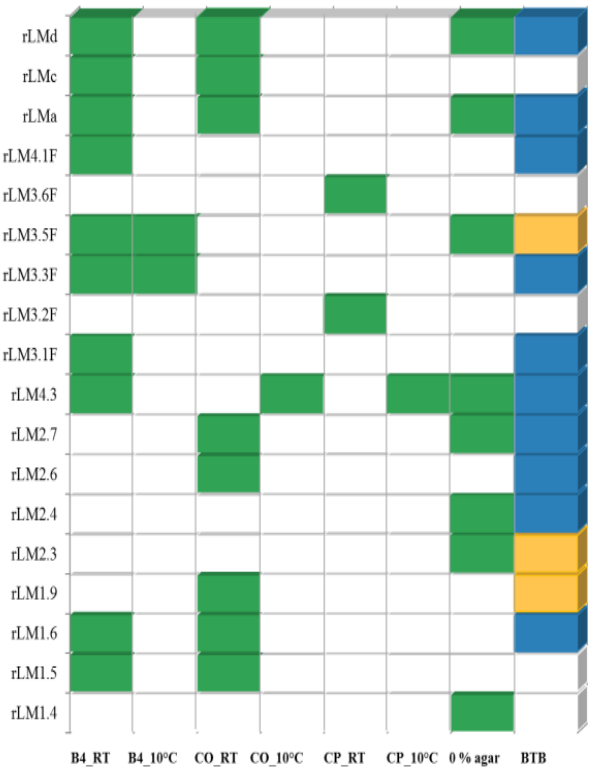

Figure 1: Mineral formation by all strains tested from rock of Lower Muschelkalk. The media used were B-4 with calcium acetate or B-4 with calcium carbonate (B4-CO) or calcium phosphate (B4-CP), all tested at 28°C or 10°C, and liquid B-4medium at 28 °C. Changes in pH were visualized on indicator plates (BTB) with yellow for change to acidic and blue for change to alkaline pH. Crystal formation is indicated in green, no crystal formation in white. See text for more details.

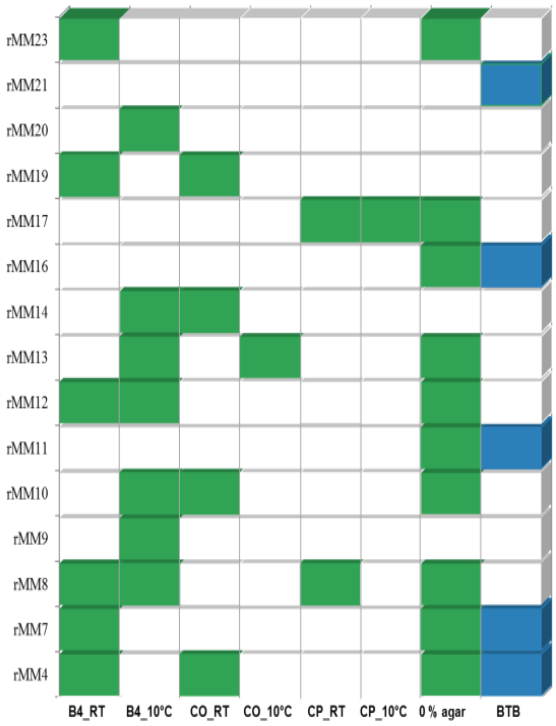

Figure 2: Mineral formation by all strains tested from rock of Middle Muschelkalk. See legend of Fig. 1 for details.

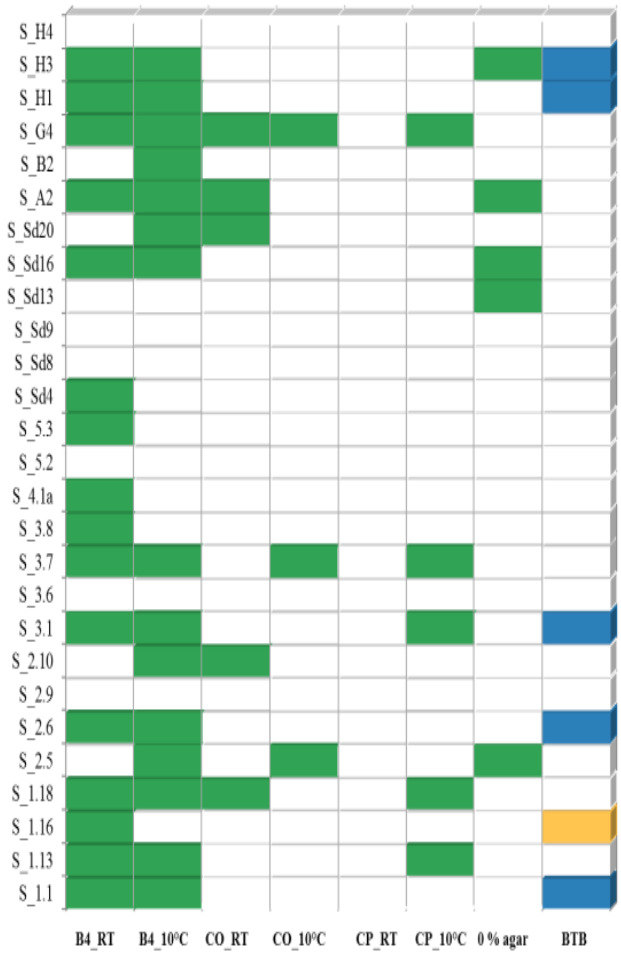

Figure 3: Mineral formation by all strains tested from groundwater in Stöben, Lower Muschelkalk. See legend of Fig. 1 for details.

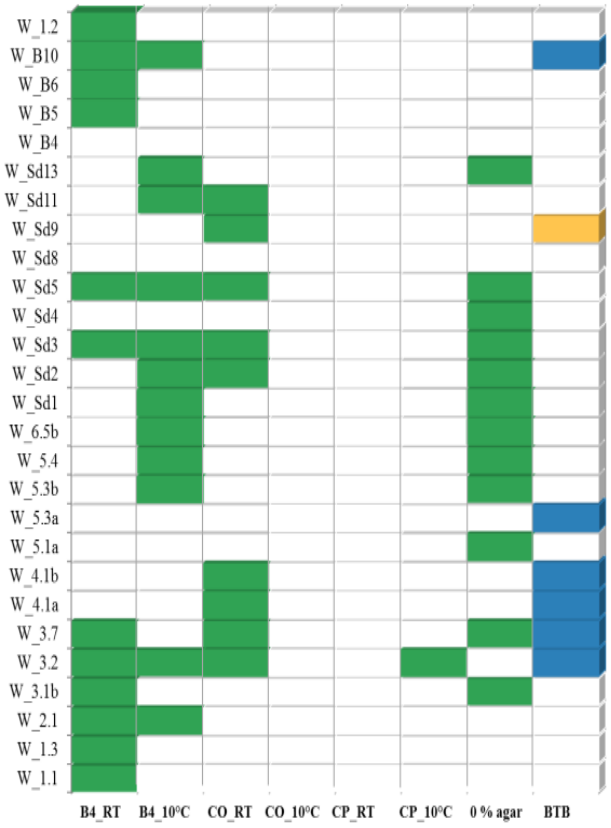

Figure 4: Mineral formation by all strains tested from groundwater in Wichmar, Middle Muschelkalk. See legend of Fig. 1 for details.

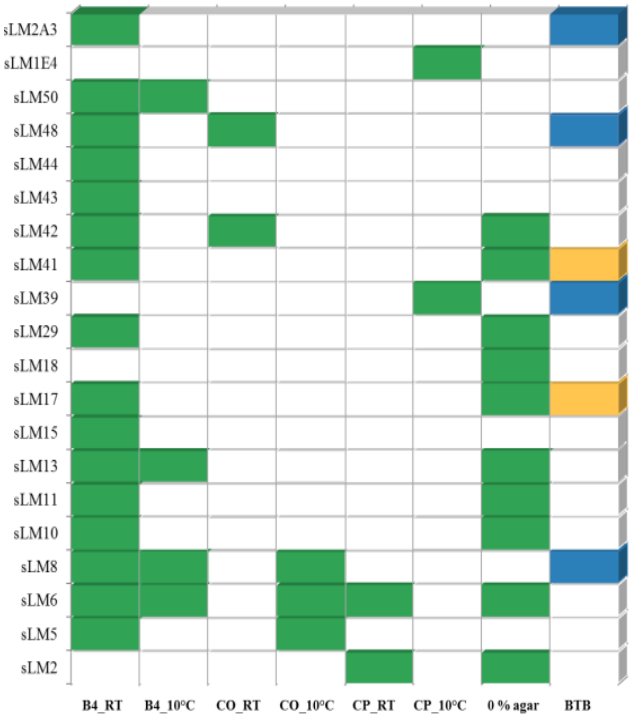

Figure 5: Mineral formation by all strains tested from soil on Lower Muschelkalk. See legend of Fig. 1 for details.

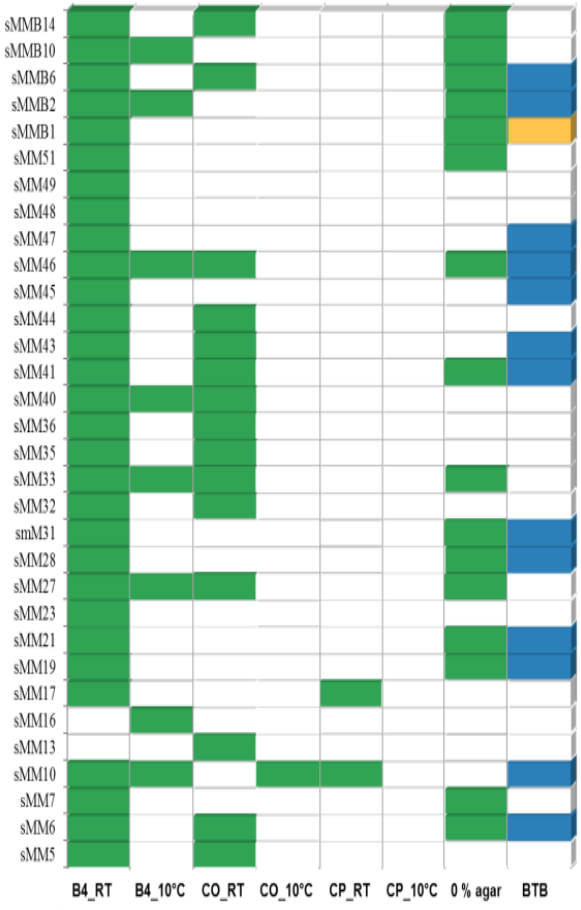

Figure 6: Mineral formation by all strains tested from soil on Middle Muschelkalk. See legend of Fig. 1 for details.

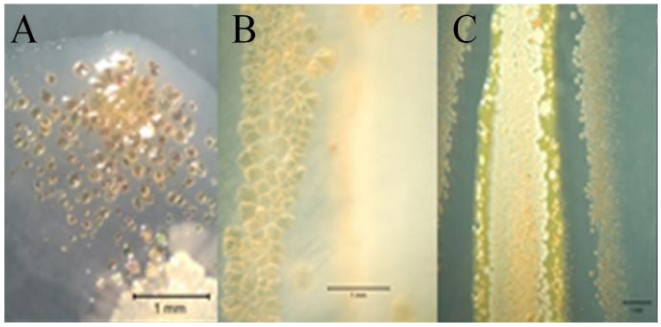

Figure 7: Crystal morphologies and distribution shown for selected strains. From Middle Muschelkalk rock *Bacillus sp.* rMM8 formed brownish spherical crystals within the agar (A), from groundwater of Lower Muschelkalk at Stöben *Lelliottia amnigena* S_H3 was recorded with brownish spherical crystals next to the culture (B), while from groundwater from Middle Muschelkalk at Wichmar *Arthrobacter sp.* W_2.1 showed a white crusts on the culture surface and reddish spherical crystals behind an inhibition zone (C).

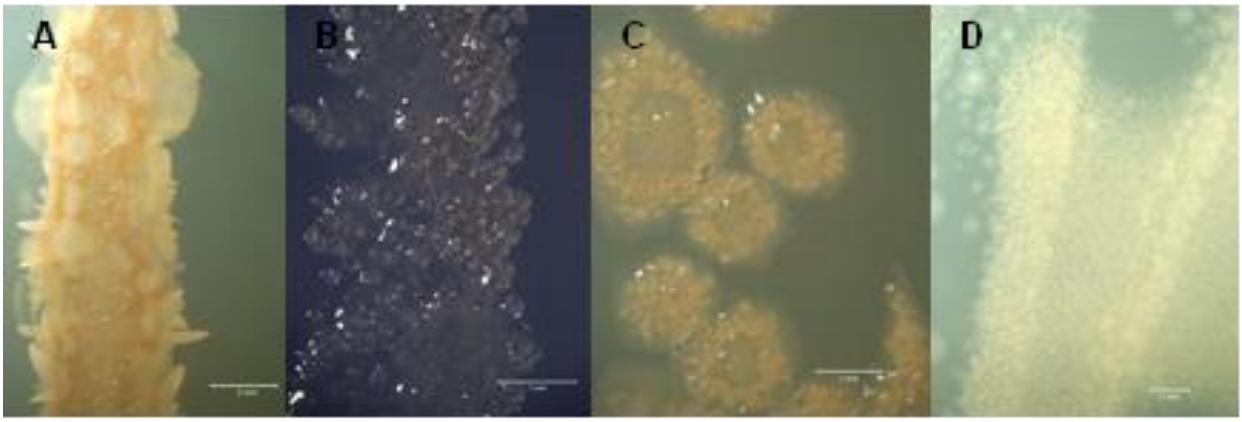

Figure 8: Mineral morphology is changed by growth temperature. *Pseudomonas sp*. S_1.1 at 28 °C (A) and 10 °C (B) shows not only induction of pigment formation, but also change from laminated shapes to transparent spheres. *Rahnella sp.* S_H1 at 28 °C forms rhombohedric to rosette like crystals at higher temperature (C), while small spheres are formed at 10 °C (D). Size bar, 1 mm.

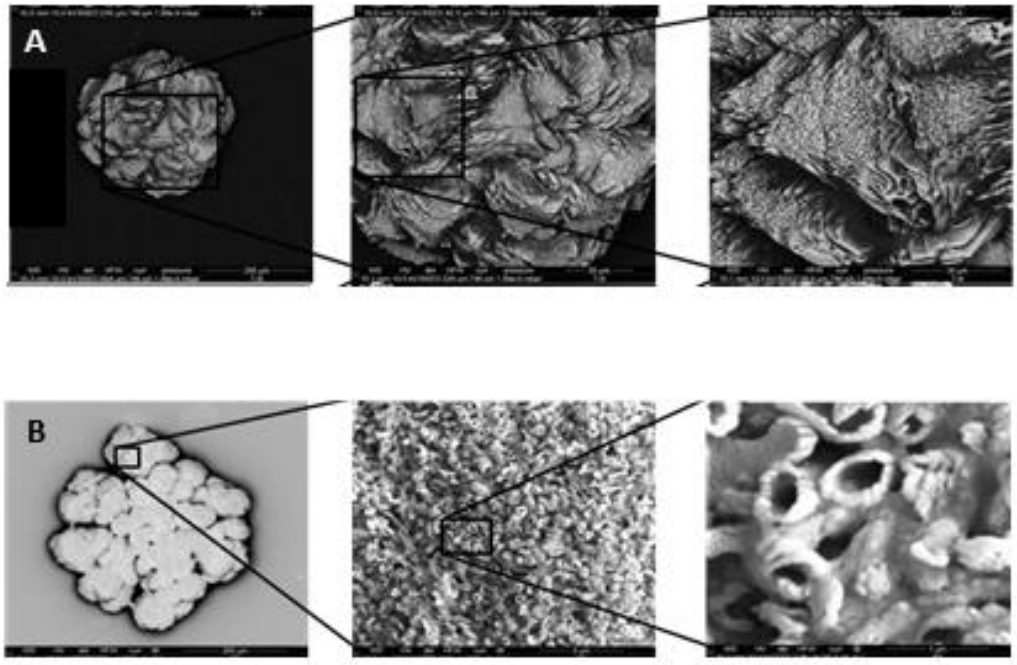

Figure 9: Scanning electron micrographs for crystal morphologies of minerals formed by *Lelliottia amnigena* S_H3 (panel A) and *Rhodococcus erythropolis* W_Sd5 (panel B), each illustrated at different magnifications. While the left images show the macromorphology, the detailed pictures give insight into surface and microcrystalline structures.